

Semi-annual Report
January - June 1997

Michael D. King and Si-Chee Tsay
Goddard Space Flight Center
Greenbelt, MD 20771

Abstract

Our major achievements of the past six months were: (i) the progress of the MOD_PR06OD V2 algorithm delivery, including the utilization of cloud mask information, (ii) the completion of file specifications for the combined MOD06 product, (iii) progress of Level-3 file specification and aggregations, quality assurance plan, and ancillary data files, (iv) the improvements of MAS-50 channel data processing and archiving, (v) the intercomparison of MAS and AVIRIS radiometric data in the shortwave region, and (vi) the analysis of cloud properties retrieval over highly reflecting surfaces.

I. Task Objectives

With the use of related airborne instrumentation, such as the MODIS Airborne Simulator (MAS) and Cloud Absorption Radiometer (CAR) in intensive field experiments, our primary objective is to extend and expand algorithms for retrieving the optical thickness and effective radius of clouds from radiation measurements to be obtained from the Moderate Resolution Imaging Spectroradiometer (MODIS). The secondary objective is to obtain an enhanced knowledge of surface angular and spectral properties that can be inferred from airborne directional radiance measurements.

II. Work Accomplished

a. MODIS-related Algorithm Study

Our work on the MODIS cloud retrieval (MOD_PR06OD V2) algorithm delivery is progressing. In particular, seven MODIS bands (0.65, 0.86, 1.24, 1.64, 2.13, 3.75, and 11.03 μm) for cloud retrievals have been synthesized into the code and restructured for optimal performance. This code will retrieve cloud optical thickness by using different MODIS bands for different surface types (0.65 μm over land, 0.86 μm over ocean, and 1.24 μm over snow/ice) at the pixel level and optical thickness will be reported at 0.65 μm . An input parameter for cloud top pressure has been added in order to make corrections for Rayleigh scattering when the 0.65 μm channel is used over land. Similarly, the input structure for atmospheric transmittance corrections for gaseous absorption and emission above the cloud has been implemented in the code. New programs to handle MODIS cloud mask information, including interfaces provided by SDST, have also been developed and integrated, which is critical to the cloud retrieval decision tree. First-cut logic and code structure were incorporated to retrieve either water-

cloud or ice-cloud parameters at the pixel level. Accordingly, new lookup libraries (reflectance and flux parameters) for seven channels of MODIS were generated for both water and ice clouds for the V2 delivery.

The ice cloud optical and microphysical properties data (ice scattering phase function, single scattering albedo, and mean effective size) were provided by Prof. K. N. Liou's group at the University of Utah. In computing the single-scattering properties of ice clouds, an updated data set of ice refractive index (Goss et al. 1996) was used. In some wavelengths, the new data deviate from the commonly used data compiled by Warren (1984), by as much as 60%. The mean refractive index of a given MODIS channel is obtained by weighting the sensor response function and spectral solar (or thermal) energy. We performed general algorithm tests of MOD_PR06OD by using MAS ARMICAS field experiment data (see section III b) and further tests are underway. Additional constraints were added in the retrieval code to require the sensor measured reflectance at the visible (e.g., 0.65 μm) to be larger than the surface albedo value. This condition is particularly important for retrieving cloud properties over highly reflecting surfaces (e.g., snow and sea ice in the arctic), since the multiple reflection between cloud and surface increases the system reflectance at visible (or non-absorbing) channels. In turn, it leads to negative retrieved cloud optical thickness values if this constraint is not included. However, for highly inhomogeneous surface conditions, this constraint will produce biased results due to the difficulty in choosing a representative surface albedo value. More detailed study is required.

A quality assurance plan is an important element in the MODIS data reduction and is required for every level of MODIS products. It includes operational (automatic) and post-operational (manual) QA specifications. An operational approach mainly includes the run time QA, metadata and operating system information that is the responsibility of the DAAC to generate. On the other hand, a post-operational approach involves data evaluation after the data are produced, such as data validation, algorithm intercomparison, etc. Within the QA plan, the run-time QA flags that are saved within each MODIS product play the central role and reflect each product's quality assessment. For MOD06OD, the run time QA includes the QA flags and QA metadata. The former is stored at the spatial resolution of 1×1 km and includes the first byte of the cloud mask, the product quality flags and the retrieval processing flags. The cloud mask QA is derived from the first byte of the MOD35 product and includes information on cloudy/clear sky determination, day/night status, sun glint, snow/ice and land/sea flags. The product quality flags provide the quality information on each retrieved parameter, and the retrieval processing flags mainly provide the input resources of ancillary data used in processing the MODIS product. In comparison, the QA metadata is designed on the basis of a granule and has some constraints from the product system. It is formed by two parts, i.e., the QA Inventory Metadata (including ECS core QA metadata and product specific QA metadata) and the Product-Specific QA Archive Metadata. The inventory metadata will be stored on-line to enhance the data searching ability. The ar-

chive QA metadata, however, will be saved only on tape and used to provide more statistical information that is not necessary to be on-line.

The ancillary data and other MODIS product data are required by the MOD06OD cloud retrieval algorithm. NCEP and DAO will be the primary ancillary data resources unless they don't have the parameters we require. In this case, MODIS products or climate values will be used. From a data source point of view, we need to read and interpolate model data (DAO or NCEP), MODIS products (05, 06, 07 and 43), Built-in Standard atmospheres (as fail-safe bucket) and NASA Langley CERES' global BRDF map. From a parameter point of view, we need the total precipitable water (g cm^{-2}) above a cloud layer, the mean temperature above the cloud layer, cloud top height, land and ocean surface temperature, BRDF/Albedo and perhaps ozone. Components completed thus far include: (i) creation of an HDF template for all MOD06 ancillary data products, (ii) computation of the mixing ratio profile from the dew point temperature profile, (iii) performing a nearest neighbor search in 2-D, (iv) reformatting CERES BRDF products to accommodate MODIS grids, and (v) preparing five standard atmospheric profiles including temperature and water vapor. In this whole process, an efficient scheme for searching the data at each MODIS field of view (FOV) is very critical. After carefully balancing between code efficiency and time/effort required by code developers, a new structure was developed based on the current version of the MOD06OD code to achieve an efficient search and interfaces. A reader for DAO sample data was also created. The integration and testing of ancillary processing is currently underway.

We have completed and submitted to SDST the file specification for the combined MOD06 product and added the HDF-EOS information and metadata to the CDL (network Common data form Description Language) version of the file specification. Preparation for the Level-3 file specification is underway. We have finalized the statistics and approaches to be used for Level-3 aggregations for each Level-3 parameter. They are the daily, 8-day, and monthly Level-3 products. The statistics include simple statistics, log statistics, fraction, regression, histogram, and joint histograms. This list of Level-3 parameters was based on inputs from all MODIS Atmosphere team members as well as a number of scientists from the GCM community.

Development is underway to create codes for performing space-time aggregation of MODIS atmosphere products, i.e., codes to produce Level-3 daily gridded files from a collection of Level-2 granules. These codes will be used to aggregate all products (e.g., aerosol over land and ocean, water vapor, clouds, and ozone amount, etc.) in the Atmosphere Group. Although the computation of aggregate quantities (i.e., mean and standard deviation) on a regular grid is a relatively simple task conceptually, the mechanics of writing general, maintainable codes has proven to be quite involved. Roughly 10% of the codes perform the computations; the rest is devoted to bookkeeping, I/O, etc. We chose to implement the aggregation codes in Fortran 90, which has allowed us to make use of the lan-

guage's extensive facilities for array processing and a variety of object-oriented features. These codes are designed to be both flexible and easy to modify. It makes extensive use of the self-documenting nature of the HDF files in which MODIS data are stored.

b. MODIS-related Instrumental Research

To assure good quality MAS 50-channel data in the shortwave region, we have conducted extensive intercomparisons between MAS and AVIRIS measurements from two recent field experiments, viz., SCAR-B (Smoke, Clouds, And Radiation-Brazil, August-September 1995) and ARM-CAS (Arctic Radiation Measurements in Column Atmosphere-surface System, Alaska, June 1995). Different types of scenes with large dynamical ranges, such as no cloud, partly cloudy, and mostly cloudy (very bright) scenes, were chosen as representative test datasets. For each target the average radiance was computed for all MAS 25 shortwave bands and the AVIRIS radiances were convolved into corresponding MAS band shapes. Two important conclusions can be drawn from this exercise: (i) MAS data, particularly for bands 1-9 (port 1), are often offset higher than AVIRIS data, especially over scenes that are very bright (such as over areas of extensive clouds or arctic sea ice). The port 1 offset peaks at band 7 (0.865 μm). Offsets in bands 10-25 (port 2) during ARM-CAS showed little change regardless of scene type, although they do appear slightly higher for SCAR-B over bright scenes. (ii) Instrument temperature appears to have some effects on the slope values of the comparisons, as evidenced by relative changes in slope values across the different bands.

The pattern of change across port 1 matches the expected sensitivity of silicon bands to temperature change. Due to the nature of this type of comparison, it is not conclusive as to whether MAS or AVIRIS (or both) are responsible for the differences noted, though there is some suggestion that the temperature correction used in the MAS processing may not be fully modeling the MAS thermal responsivity. Results from these comparisons were discussed with Ames personnel. It was suggested that some of the differences between MAS and AVIRIS, particularly over bright targets, could be due either to light leakage in the MAS optics, in the AVIRIS dark source, or both. Some laboratory tests were conducted at Ames to simulate the higher offset over bright scenes as noted. After analyzing these measurements, we find that stray light from outside the direct field of view of the MAS is minor.

In addition, we have reviewed possible cases for 1996 MAS-AVIRIS comparisons. Because there were many instrumental changes in the MAS in early 1996, data obtained following these changes were analyzed to see if the same effects observed in 1995 (ARM-CAS and SCAR-B) were still present. Data from 7 July and 30 July 1996 were analyzed using a similar procedure as that used in 1995 comparisons. AVIRIS data were obtained from JPL and integrated over the MAS bandwidths (updated for 1996) and converted to a similar spatial resolution as

the MAS. Results of this analysis show some difference in slopes but the intercept differences are still similar to 1995 results. Thus, while it is unknown from this type of analysis the cause of the disagreement between the two instruments, it does demonstrate that upgrades performed to the MAS between 1995 and 1996 had little or no effect on the rather substantial offset differences noted in certain cases between the two instruments.

In an effort to standardize the MAS operations, a document was discussed and drafted by Goddard, Ames and University of Wisconsin scientists to lay out the status of the instrument both now and for the future, and to define calibration roles and analysis of MAS thermal chamber data. Ames personnel have particularly requested assistance in analyzing MAS thermal chamber calibration data.

c. *MODIS-related Services*

Meetings

1. Xu Liang, Ran Song, and Menghua Wang attended the MODIS Level-3 module process meeting, held at Goddard, on 24-25 February 1997. Dr. Liang presented a preliminary study on wavelets and their application to aerosol data;

2. Si-Chee Tsay attended the Conference on Weather Analysis and Forecasting, Taipei, Taiwan, on 3-7 March 1997, and presented an update on EOS remote sensing and retrievals of atmospheric aerosols and clouds;

3. Steve Platnick and Michael King regularly attended weekly MODIS Technical Team meetings.

4. Michael King attended the *Topical Meeting on the Optical Remote Sensing of the Atmosphere*, Santa Fe, NM, on February 10-13, where he gave an invited talk entitled: "Remote sensing of cloud, aerosol, and water vapor properties from the Moderate Resolution Imaging Spectroradiometer (MODIS)."

5. Michael King attended the Department of Energy Atmospheric Radiation Measurement (ARM) meeting in San Antonio, TX, on 4-6 March 1997, where he participated in a panel discussion on EOS/ARM interactions, especially as it relates to validation.

6. Steve Platnick attended the 15th CERES Science Team meeting, held at NASA Langley Research Center, Hampton, VA, on 16-19 April 1997, where he presented recent results from MODIS cloud retrieval algorithm studies.

7. Michael King, Xu Liang, Steve Platnick, Ran Song, Si-Chee Tsay, and Menghua Wang attended the MODIS Science Team meeting, held at College Park, MD, on 14-15 May 1997, where Xu Liang presented "Level-3 design and development plans" in the Atmosphere group meeting.

8. Michael King, Robert Pincus, and Xu Liang attended the AGU Spring Meeting, held in Baltimore, MD, on 27-30 May 1997, where Robert Pincus presented "In situ measurements of the absorption of solar radiation by stratiform water clouds," Xu Liang presented "Intercomparison of land surface schemes using large scale data," and Michael King presented "Radiative properties of smoke, clouds, and aerosol over land surfaces in Brazil: Airborne observations."

9. Michael King, Tom Arnold, and Steve Platnick attended a two-day meeting on MAS calibration and instrument status, held at NASA Ames Research Center, including Ames and University of Wisconsin personnel to discuss the current instrument and calibration status, define roles (particularly for the calibration) and discuss future plans.

Seminars

1. King, M. D., "NASA's Mission to Planet Earth," at Amundsen-Scott South Pole Station (January).

2. Pincus, R., "In situ measurements of the absorption of solar radiation by stratiform water clouds," at the Geophysical Fluid Dynamic Laboratory, Princeton, New Jersey (January), at NASA Langley Research Center, Hampton, Virginia (March), and at NASA Goddard Space Flight Center, Greenbelt, Maryland (June) 1997.

3. Pincus, R., "Lumpy clouds: Understanding spatial and temporal variability in marine stratocumulus," Columbia University/NASA Goddard Institute for Space Studies Graduate Student Seminar Series, New York, January 1997.

4. Pincus, R., "Radiative processes in boundary layer clouds: Models and observations from satellites, aircraft, and ships," at NOAA Office of Research and Applications, Silver Spring, Maryland, April 1997.

III. Data/Analysis/Interpretation

a. Data Processing

Data processing, with final calibration, of MAS Level-1B data was completed for all nine ARMCAS flights. This new version of MAS data is no longer inventoried in slices. Individual flight tracks are now tagged by date and flight track number. A new set of browse images and summary statistics have been attached to the MAS Web site (<http://ltpwww.gsfc.nasa.gov/MAS>). In addition, new in-line thumbnail images (linked to larger/higher resolution images) of the flight pattern are provided for individual MAS missions. These thumbnail maps should assist MAS data users in selecting interesting mission days quickly. Interested users can obtain a copy of these data by contacting the Goddard DAAC (Pat Hrubiak at hrubiak@daac.gsfc.nasa.gov) and request the data in either Digital Linear Tape (DLT) or Exabyte 8500 tape. Typical Level-1B HDF output

files vary between 100 and 800 megabytes. The SCAR-B Level-1B processing (version 9) with final calibration has been completed for the first four flights: 16, 18, 20, and 23 August 1995.

Recent field campaigns of SUCCESS (SUBsonic aircraft: Contrail and Cloud Effects Special Study, Kansas, April-May 1996), TARFOX (Tropospheric Aerosol Radiative Forcing Observational eXperiment, Wallops Island, Virginia, July 1996), and WINCE (WINter Cloud Experiment, Wisconsin, February 1997) adopted the "Golden Day" concept whereby preliminary calibration coefficients were adopted for quick data processing shortly after the completion of the experiment. For example, the WINCE Level-1B HDF data for 3 selected golden days (6, 9, 12 February 1997) are now available from the Goddard DAAC. All browse images and flight track summary statistics are available from the MAS WWW site.

The MAS web site has been redesigned. Highlights of the changes are: as follows:

- Updated the Home page with new imagery
 - A new ER-2 aircraft image (click on image to load full-resolution version)
 - A GIF animation of some new MAS Earth Scenes
 - Updated sub-page link buttons
- Changed the beveled-button links on the Gallery, Reference, and Data pages to drop-shadow image links. Created new thumbnail campaign logo links on the Data page.
- Added a consistent beige-stripe background to all pages. This should aid visitors with site recognition (to help visitors know the instant they have left the MAS site). The home page has a larger stripe to emphasize that it's the top-level (subject-wise) page.
- Added consistent Title/Navigation bars to all pages
 - Every page now has a Home page source identification and link. (The top-most title bar). This is important since search engines can (and often do) link visitors to a lower level page of a site. Now surfers can "click" on the tile bar on any page to return to the home page.
 - Title bars under the Home page bar show the names of and offer links to the referring pages within the MAS site structure. This should help visitors know where they are within the structure of the site, and gives them an easy way to return to a higher level.
- Added subsections of better high-resolution images to the Earth Scene Exhi-

bition page (linked from the Gallery page).

Figure 1 shows a composite of MAS imagery constructed from various field campaigns, and was selected as the cover page for the June issue of *Photogrammetric Engineering and Remote Sensing* (PE & RS). A low resolution (75 dpi) version of the image appeared on the journal cover.

The Web site for CAR (<http://climate.gsfc.nasa.gov/CAR>) was recently established, and it serves as an information center for the CAR data user community. A new CAR web page for ARMCAS data (e.g., quicklook images, flight information, etc.) has recently been completed, and it contains numerous design improvements over previous versions. The CAR HDF processing will soon be upgraded from Fortran 77 to Fortran 90. This is necessary because CAR HDF processing demands certain programming features that are not offered in the Fortran

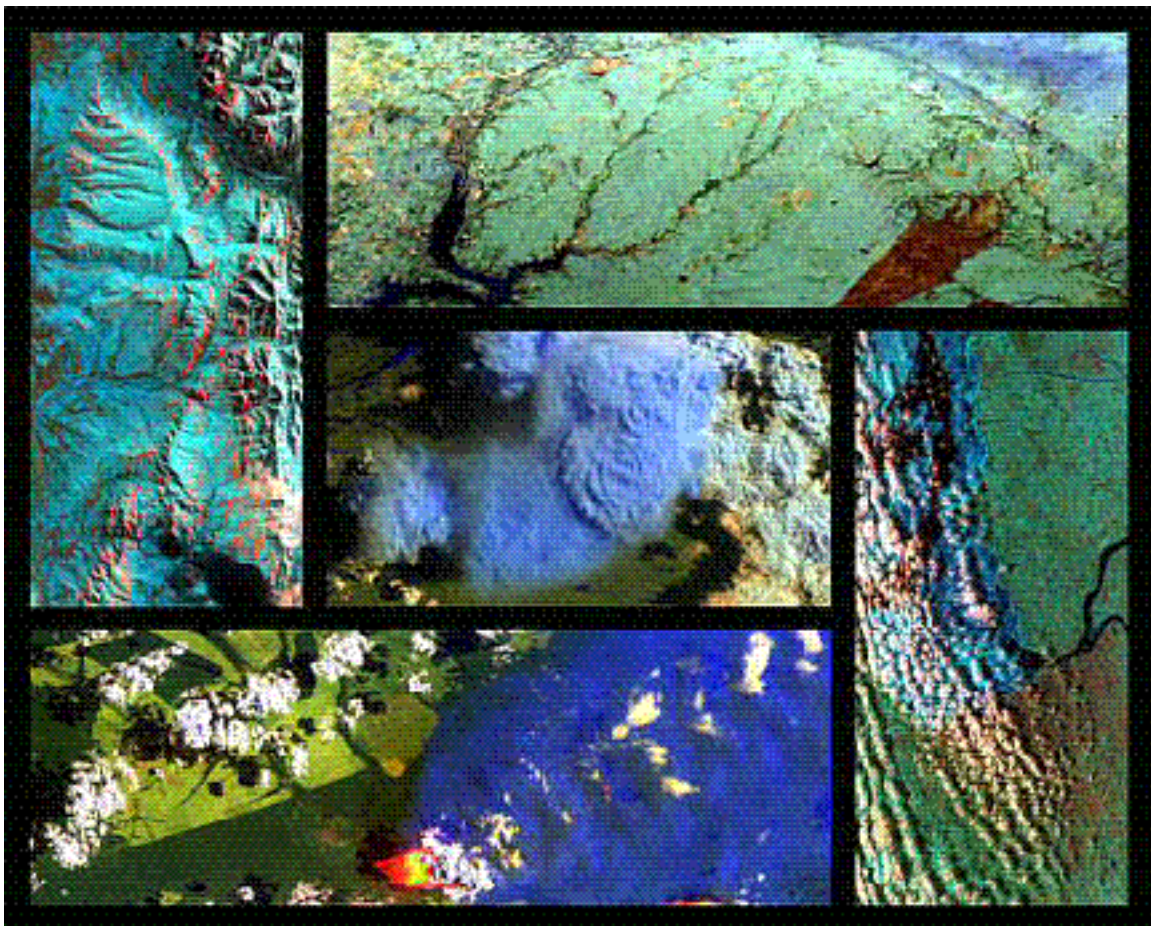


Figure 1. Clockwise from the upper left (center last) the images depict: (a) Glaciers, ice, and snow just north of Mt. Hayes in the Alaska Range (Alaska-April95 Campaign); (b) Arkansas River and Kaw Reservoir near the Kansas/Oklahoma border (SUCCESS Campaign); (c) Lake-effect clouds and snow from Lake Erie into Buffalo, New York (WINCE Campaign); (d) Tropical biomass burning and smoke plume near the Xingu River, Brazil (SCAR-B Campaign); and (e) Severe thunderstorm over the Brooks Range, Alaska (ARMCAS Campaign).

77 implementation but are now available in Fortran 90, features such as dynamic memory allocation, derived data types, and pointers, etc.

New data from the UV calibration, conducted in December 1996, were processed and analyzed to infer calibration slope and intercept values. All SCAR-B and ARM-CAS CAR data, including the UV-B channel, have been reprocessed into HDF and a much improved version of quicklook images was produced that presents six bands-worth of radiometric information simultaneously. A read Car-Data subroutine is also provided, which interfaces with the CAR HDF data objects and returns radiance (in units of $\text{W m}^{-2} \text{sr}^{-1} \mu\text{m}^{-1}$), scan angles of each pixel, solar zenith and azimuth angle, aircraft heading, etc. With these useful parameters, a CAR HDF data user can compute BRDFs without a need to know details of the HDF data structure.

b. Analysis and Interpretation

Retrieving cloud properties over highly reflecting surfaces is not a trivial task, since the multiple reflection between cloud and surface increases the system reflectance at all non-absorbing channels. This in turn reduces the sensitivity on retrieving cloud properties or increases the possibility of getting multi-valued solutions. The ARM-CAS measurements were designed to acquire data for testing our cloud retrieval algorithm over highly reflecting surfaces. An example of test results is discussed below. Figure 2 shows the time and location of ER-2 (MAS swaths) and the collocated NOAA-12 (AVHRR) measurements. The cloud fields around the MAS swaths are relatively uniform and single-layered stratiform clouds (also identified clearly from Cloud Lidar System data, not shown).

In addition, the University of Washington's C-131A and ER-2 flight tracks were

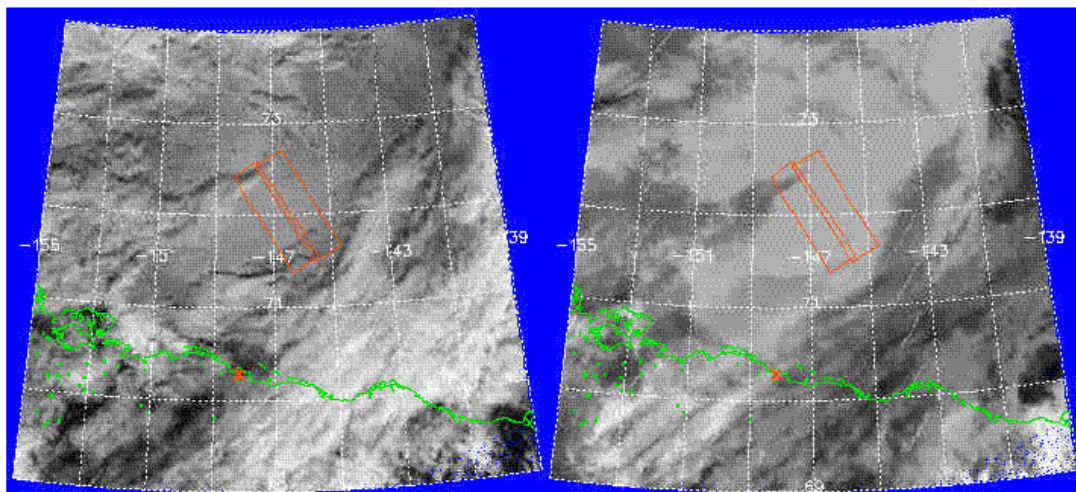


Figure 2. NOAA-12 AVHRR images obtained over the Beaufort Sea, Alaska on 14 June 1995 during the ARM-CAS experiment (2114 UTC). Superimposed on these images are MAS swaths for two ER-2 ground tracks obtained between 2100 and 2150 UTC (red boxes). The AVHRR image on the left was obtained in channel 2 ($0.87 \mu\text{m}$) and the image on the right at channel 4 ($11 \mu\text{m}$).

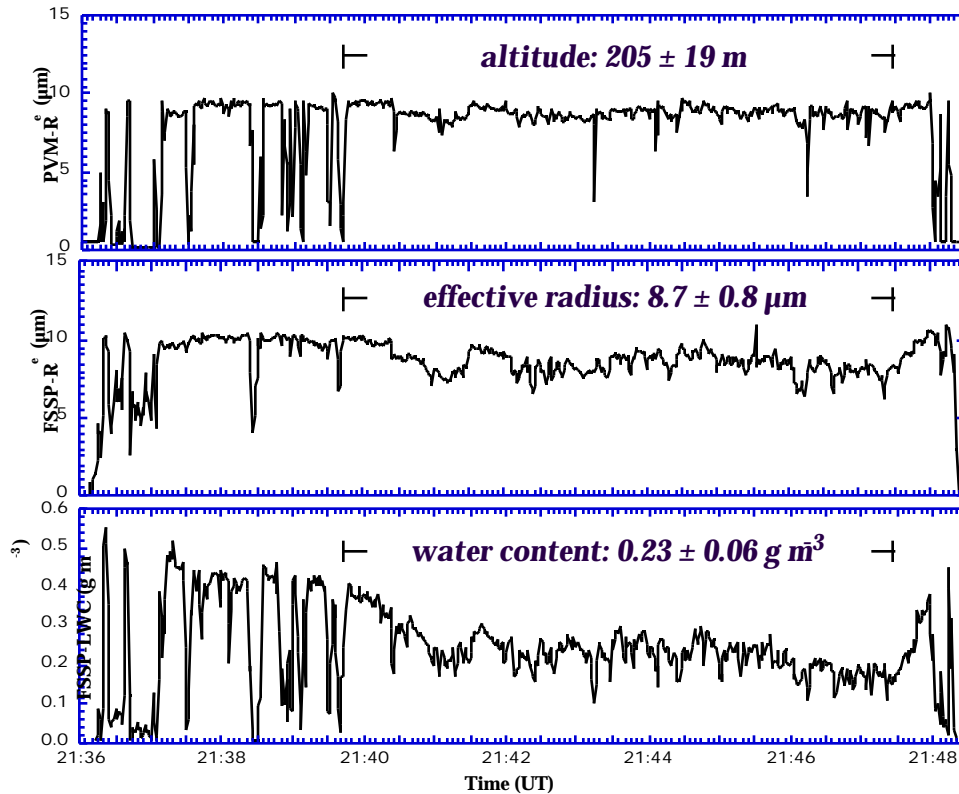


Figure 3. Time series of in situ microphysics data obtained from the University of Washington C-131A aircraft between 2136 and 2148 UTC on 14 June 1995.

created for that particular day to pin down the best coordinated period for analyzing measured microphysical parameters (such as drop concentration, effective radius, liquid water content) from various probes. The microphysics data are depicted in Fig. 3, along with a summary of statistics. This stratus deck appeared fairly uniform, relatively constant in effective radius and liquid water content at the altitude of about 200 m, which is an ideal case for cloud retrieval study.

The retrieved results are presented in Fig. 4. Two surface albedo values of sea ice were assumed at the visible channels (0.5 and 0.6 μm), which were the ranges inferred from CAR measurements. The *in situ* mean droplet radius is well-bounded between the retrieved effective particle radii. The standard deviation of measured droplet radius is larger than that in Fig. 3, due to an increase of sample size. However, the mean value did not change. Assuming a surface albedo of 0.5 at $\lambda = 0.67 \mu\text{m}$, there were less than 4% of the data not processed, as opposed to $\sim 30\%$ when a surface albedo of 0.6 was assumed. By proper adjustment of surface albedo, a good agreement of retrieved and measured effective particle radius can be reached. This clearly demonstrates the importance of accurate measurements of surface albedo in the polar regions, or the drawback of the algorithms depending on this channel for retrievals. Action is currently underway to study the utilization of the MODIS 1.24 μm channel as a replacement for 0.67 μm for cloud optical thickness retrievals in polar regions.

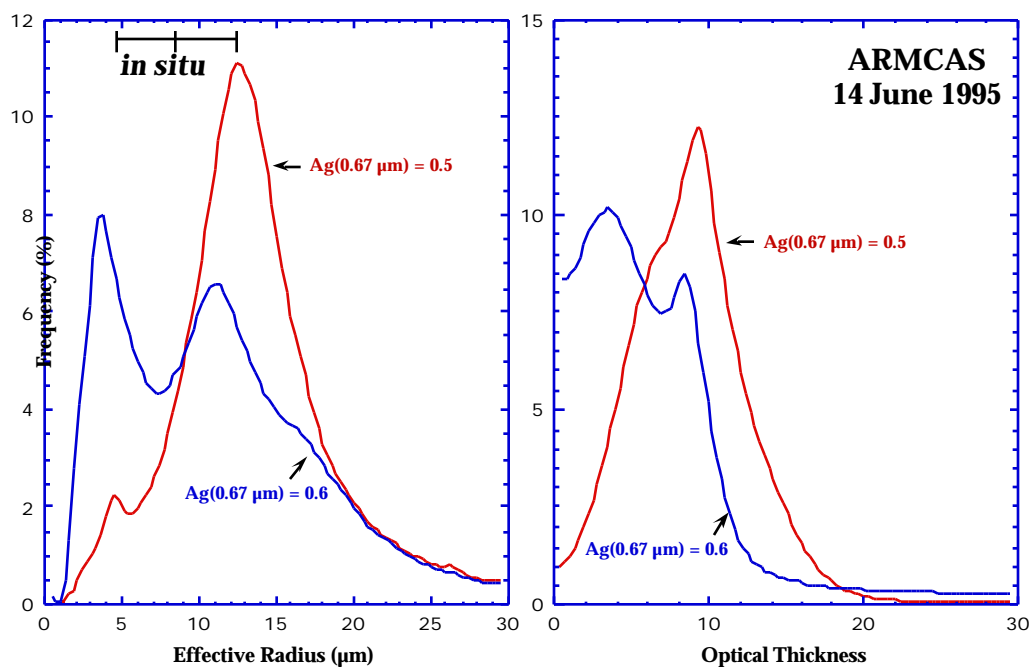


Figure 4. Marginal probability density function for effective particle radius (left) and cloud optical thickness (right) for two different assumptions on the surface albedo of the underlying sea ice. The red (blue) curves are when the surface albedo was assumed to be 0.5 (0.6). The mean and interquartile range of in situ measurements of effective radius are shown on the left hand figure for comparison purposes.

IV. Anticipated Future Actions

- a. Continue to work on the MODIS v2 cloud retrieval algorithm delivery, including the cloud mask interface, ice/water cloud logic tree, and QA flags;
- b. Extend and refine retrieval libraries to include ice cloud models for the MODIS v2 software delivery;
- c. Continue to analyze MAS, AVIRIS, and CLS data gathered during the ARMCAS campaign, as well as AVHRR, University of Washington C-131A in situ data, and surface data, all with the express purpose of helping to develop the MODIS cloud masking algorithm;
- d. Continue to analyze MAS, AVIRIS, and CLS data gathered during the US-Brazil SCAR-B campaign, as well as University of Washington C-131A in situ and radiation data to study aerosol mask and aerosol-cloud interactions;
- e. Continue to analyze surface bidirectional reflectance measurements obtained by the CAR during the Kuwait Oil Fire, LEADEX, ASTEX, SCAR-A, ARMCAS, SCAR-B, and TARFOX experiments;

f. Attend the CERES (16-18 September) and MODIS (22-24 October) science team meetings to be held at Oregon State University, Corvallis, OR, and Goddard Space Flight Center, respectively.

g. Attend the Earth Observation and Environmental Information conference (13-16 October) in Alexandria, Egypt.

V. Problems/Corrective Actions

No problems that we are aware of at this time.

VI. Publications

1. Kaufman, Y. J., D. Tanré, H. R. Gordon, T. Nakajima, J. Lenoble, R. Frouin, H. Grassl, B. M. Herman, M. D. King and P. M. Teillet, 1997: Passive remote sensing of tropospheric aerosol and atmospheric correction for the aerosol effect. *J. Geophys. Res.*, **102**, 16815–16830.

2. Platnick, S., P. A. Durkee, K. Nielson, J. P. Taylor, S. C. Tsay, M. D. King, R. J. Ferek, P. V. Hobbs and J. W. Rottman, 1997: The role of background cloud microphysics in the radiative formation of ship tracks. *J. Atmos. Sci.*, in press.

3. Wang, M., and M. D. King, 1997: Correction of Rayleigh scattering effects in cloud optical thickness retrievals. *J. Geophys. Res.*, in press.

4. Li, J. Y., H. G. Meyer, G. T. Arnold, S. C. Tsay, and M. D. King, 1997: *The Cloud Absorption Radiometer HDF Data User's Guide*. NASA Technical Memorandum 104643, 34 pp.

5. Pincus, R., S. Platnick and M. D. King, 1997: In situ measurements of the absorption of solar radiation by stratiform water clouds. *J. Atmos. Sci.*, submitted.

6. King, M. D., S. C. Tsay and S. A. Ackerman, 1997: MODIS Airborne Simulator: Radiative properties of smoke and clouds during ARM-CAS and SCAR-B. *Proc. Third International Airborne Remote Sensing Conference and Exhibition*, Copenhagen, Denmark.

7. Soulen, P. F., R. Pincus, S. C. Tsay and M. D. King, 1997: Cloud Absorption Radiometer: Airborne measurements of clouds and surface reflectance. *Proc. Third International Airborne Remote Sensing Conference and Exhibition*, Copenhagen, Denmark.

8. Kaufman, Y. J., P. V. Hobbs, V. W. J. H. Kirchhoff, P. Artaxo, M. D. King and D. Ward, 1998: Overview of the SCAR-B experiment. *J. Geophys. Res.*, in preparation.

9. King, M. D., Y. J. Kaufman, D. Tanré and T. Nakajima, 1997: Remote

sensing of tropospheric aerosols from space: Past, present, and future. *Bull. Amer. Meteor. Soc.*, in preparation.